

The effects of inter-bar currents in cast aluminium and cast copper rotors

Alexander Stening, Chandur Sadarangani
 Department of Electrical Machines and Power Electronics
 Royal Institute of Technology,
 Teknikringen 33, 100 44 Stockholm, Sweden,
 e-mail: alexander.stening@ee.kth.se

Abstract- In this paper, a study of the influence of inter-bar currents on induction machines with aluminium and copper casted rotors is presented. The resistance between the rotor bars and the iron core is measured on five different rotors. An analytical model to predict the influence of inter-bar currents on machine performance is developed, and the results are verified by measurements. It is found that the measured inter-bar resistance is lower in cast copper rotors than in cast aluminium rotors. This leads to a reduced pull-out torque and increased stray-load losses.

I. INTRODUCTION

Skewing of the rotor bars in induction machines is a common practice to reduce the acoustic noise arising from slotting effects. Assuming that the rotor bars are insulated and that the choice of skewing is made properly, the high frequency cage losses can be reduced. If the resistance between the bars and the iron core is low, currents will start to flow between the bars through the lamination. These currents are known as inter-bar currents. They increase the stray-load losses in the machine and they also affect the torque during start-up.

The resistivity between the rotor bars and the iron stack is referred to as inter-bar resistivity. The losses due to inter-bar currents are strongly dependent on both the inter-bar resistivity and the skewing. All skewed machines have inter-bar currents as long as the bars are not perfectly insulated.

Large motors are manufactured with fabricated aluminium or copper bar rotors. The prefabricated bars are inserted in the iron core and the short circuit rings are welded or brazed to the bars. However, this choice is unattractive for small to medium sized motors due to cost reasons. These machines are generally equipped with die cast aluminium rotors. As a result of the casting process the inter-bar resistivity becomes quite low. This promotes the flow of inter-bar currents.

Due to advancements in casting technology, it is possible to manufacture die cast copper rotors. Thanks to the higher conductivity of copper, the motor efficiency can be increased. Measurements have shown, however that the increase in efficiency is not as large as expected theoretically. The reason for this is increased stray-load losses.

This paper present a study performed on cast aluminium and cast copper rotors. The inter-bar resistance is measured on both aluminium and copper rotors. An analytical model is used to

calculate the effect of inter-bar currents on the motors starting performance. Dynamic measurements of the starting torque have been performed to verify the results.

II. MEASUREMENTS OF INTER-BAR RESISTIVITY

The casting process results in a distributed low resistive path between the rotor cage and core. To determine this resistance accurately is a difficult task. It is not possible to measure the inter-bar resistivity directly; it has to be calculated from measurements. The methods known can be categorized as “non-destructive” and “destructive” methods.

In 1958, Odok presented a method to measure inter-bar resistance on casted rotors [1]. A direct current is fed into one short-circuit ring and taken out through the shaft on the opposite side. The voltage drop between the ring and iron core is measured along the axial direction. Based on the average value of this voltage, the inter-bar resistivity is calculated. Odok also came to the important conclusion that the inter-bar impedance can be assumed to be purely resistive. Odok’s method is simple but not so accurate since it does not take the distribution of the bar currents into account.

Odok’s method was further developed, among others by Dabala in [2]. Assuming an equally distributed inter-bar resistivity, this method takes the distribution of the bar currents into account.

When casted copper rotors were introduced the measurements became even more challenging. Dabala suggested an improved method for measurements on casted copper rotors [3]. The improved method is not only taking the distribution of the bar currents into account, it also considers the resistivity of the iron sheets.

The method in [3] is used to determine the inter-bar resistivity for a set of aluminium and copper rotors. All rotors are made for the same 4-pole stator, rated at 11 kW. The geometries of the rotors are the same for both concepts.

A. Modeling of the rotor

The non-destructive method with a direct current flowing through the cage-stack-shaft path was used and illustrated in Fig. 1. The rotor was modeled with a parameter network distributed in the axial direction x , as proposed by Dabala in [3]. However, the equivalent circuit in Fig. 2 has been further

developed taking full consideration of the voltage drop along the shaft. This is obtained by the parallel connection of all the rotor bars instead of representing one bar. As a result, the boundary conditions for the current are changed. These boundaries are now given by the total current I flowing through the rotor instead of current per rotor bar. The boundary conditions can, hence, be expressed as

$$I_1(0) = I_2(L) = I, \quad (1)$$

$$I_1(L) = I_2(0) = 0, \quad (2)$$

where L is the length of the iron stack. With the total current flowing through the shaft, the corresponding voltage drop is then modelled correctly.

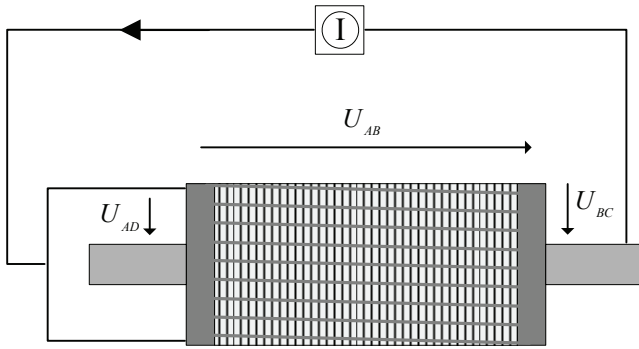


Fig. 1 Rotor test setup.

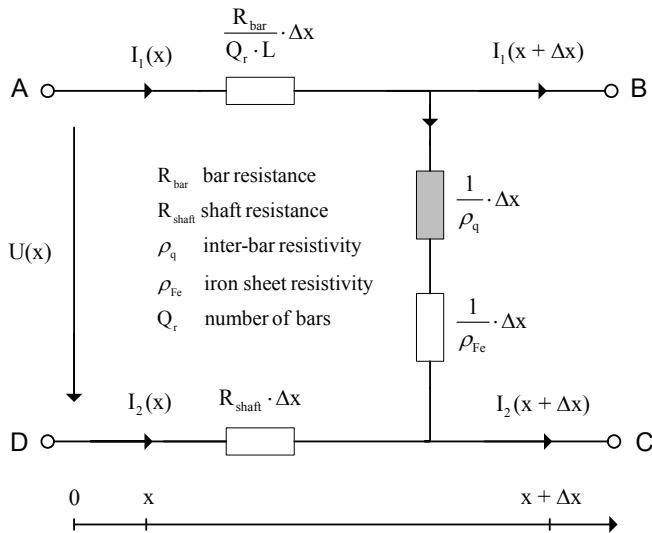


Fig. 2 Equivalent network for the rotor.

The distributed parameter network leads to a system of differential equations. This system is solved for the bar to shaft voltage U , the bar current I_1 and the shaft current I_2 . The solutions are given in the form:

$$U = U(x, \rho_q), \quad (3)$$

$$I_1 = I_1(x, \rho_q), \quad (4)$$

$$I_2 = I_2(x, \rho_q). \quad (5)$$

The ring to bar voltage U_{Ax} is then given by:

$$U_{Ax}(x, \rho_q) = \frac{R_{bar}}{Q_r \cdot L} \cdot \int_0^x I_1(x, \rho_q) \cdot dx, \quad (6)$$

and the ring to ring voltage is calculated as

$$U_{AB}(\rho_q) = U_{Ax}(L, \rho_q). \quad (7)$$

The voltages between the short-circuit rings and the corresponding shaft ends are given by

$$U_{AD}(\rho_q) = U(0, \rho_q), \quad (8)$$

and

$$U_{BC}(\rho_q) = U(L, \rho_q). \quad (9)$$

The ring-to-ring and the ring-to-shaft voltages are studied as a function of inter-bar resistivity in Fig. 3. In this case, a copper rotor with a total rotor current of 200 A is modeled.

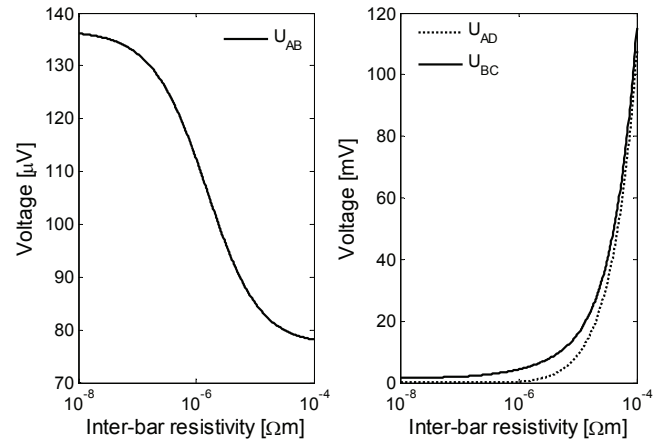


Fig. 3 Calculated voltages as a function of inter-bar resistivity for a copper rotor with a total current of 200 A.

The largest voltage, U_{BC} is expected between the ring and shaft at the end where the current is taken out from the rotor. The ring-to-ring voltage, U_{AB} , can be a good measure of the inter-bar resistivity but this voltage is sensitive to the current distribution in the bar, according to (6)-(7).

It could be noted from the measurements that the accuracy for calculating the inter-bar resistivity was poor when the change of voltage to inter-bar resistivity was low. These areas were therefore avoided in the analysis.

B. Results from measurements

A direct current of 200 A was supplied to the rotors, and the three voltages in Fig. 3 were measured. Based on these results, the inter-bar resistivity could be calculated. The determined inter-bar resistivities for five different rotors are presented in Table 1. The results show that the inter-bar resistivity is at least a factor ten lower in the casted copper rotors than in the casted aluminium rotors.

TABLE I
INTER-BAR RESISTIVITY CALCULATED FROM MEASURED VOLTAGES
AT A TOTAL ROTOR CURRENT OF 200 A.

	Inter-bar resistivity ρ_q [$\mu\Omega$ m] calculated from	
	U_{AB}/U_{AD}	U_{BC}
132 Cu 1	0.3	0.4
132 Cu 2	0.4	0.3
132 Cu 3	0.4	0.6
132 Al 1	7.0	9.0
132 Al 2	4.0	7.0

In order to verify the analytical model, the current distribution in the rotor bars is studied. The ring-to-bar voltage U_{AX} , was calculated based on the measured resistivity. In Fig. 4, the calculated voltage is compared with measured values along seven bars for a copper rotor with a total current of 100 A. The measured voltages show a good agreement with the calculated values. This implies that the current distribution in the bars is modeled correctly.

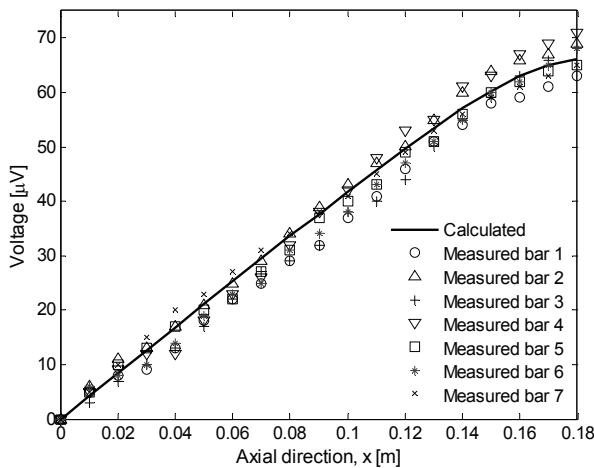


Fig. 4 Measured and calculated ring to bar voltage along 7 bars for a copper rotor at a total current of 100 A.

III. MODEL FOR ANALYSIS OF INTER-BAR CURRENTS

The analytical model used to include the effect of inter-bar currents is derived from Behdashti's work in [4]. And has been

further developed as described below. A saturation factor is introduced, taking into account saturation of the leakage paths during a start [5]. The skin effect is considered when calculating the rotor impedances [6]. The fundamental component of the stator current is calculated also taking into consideration inter-bar effects. The inter-bar resistivities calculated from the previous measurements are used as input to this model.

Starting characteristics

The inter-bar currents affect the starting performance of the machine, the amount depending on the ratio of the number of stator and rotor slots. Another important factor is the rotor skew. The 11 kW machine is simulated with both a copper and an aluminium rotor. Fig. 5 shows the torque speed characteristics for the two motor concepts.

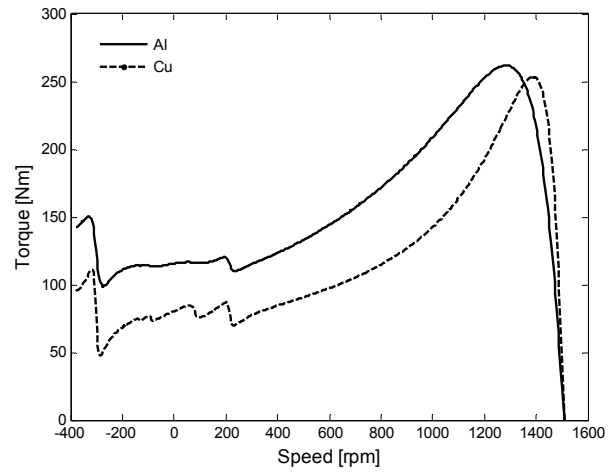


Fig. 5 Calculated torque for the 11 kW motor equipped with either an aluminium rotor or a copper rotor at 400 V.

It can be seen that the 5th and the 7th space harmonics causes asynchronous torque components which distort the torque contribution from the fundamental component. The torque of the copper rotor is more affected by the harmonics than the aluminium rotor; which is due to the inter-bar currents. However, the influence is not that large in this case thanks to a proper choice of slot numbers and skew.

If only the fundamental component is considered, the magnitudes of the pull-out torques should be exactly the same for the two rotor concepts. However, at this speed, the harmonic torques counteract the accelerating torque. The reduction of the pull-out torque in the copper rotor is therefore due to contribution of a larger harmonic torque.

The simulations show that the pull-out torque of the copper rotor is 3 % lower than the corresponding torque of the aluminium rotor. The result implies that the inter-bar currents are causing larger braking torques in the copper rotor than in the aluminium rotor, thereby creating larger inter-bar current losses. The measurements presented in the next section further reveal that these losses are even larger than calculated.

IV. TORQUE MEASUREMENTS

The torque during start-up was measured on the 11 kW machine. One aluminum rotor and one copper rotor have been tested. The torque was measured dynamically during start when the machine was loaded with a flywheel. The unfiltered torque signal was sampled at a high frequency and the signal noise in the sampled data was suppressed by the use of a low-pass butterworth filter of the 5th order with a cut-of frequency selected sufficiently high.

A. Measurement setup

A rotating torque transducer was used to measure the torque. The torque transducer, Magtrol TM-312, was mounted between the motor shaft and a flywheel. The moment of inertia of the flywheel was 1.6 kgm².

First, the motor was accelerated in reverse direction to half the synchronous speed. Then, the torque was measured after shifting two phases of the sinusoidal supply voltage, forcing the machine to accelerate in the opposite direction. By doing this, the influence of the 5th and 11th space harmonic could be measured.

B. Results from measurements

The starting torque was measured at different levels of magnetic saturation. The measured torques at a line to line voltage of 100 V is shown in Fig. 6.

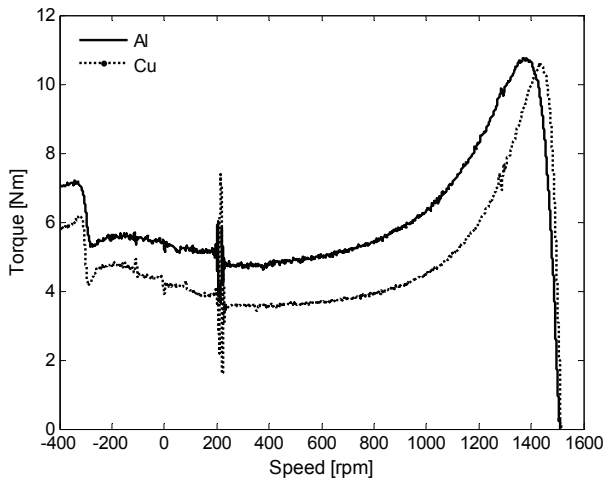


Fig. 6 Torque as a function of speed for the machine at 100 V.

At this low voltage, the rotor accelerates relatively slowly. Therefore, the frequency of the synchronous torque was low enough to pass through the filtering process. This torque occurs at the synchronous speed of the 7th space harmonic, making it difficult to observe the influence of the 7th asynchronous torque. The effect of the 5th space harmonic is more obvious.

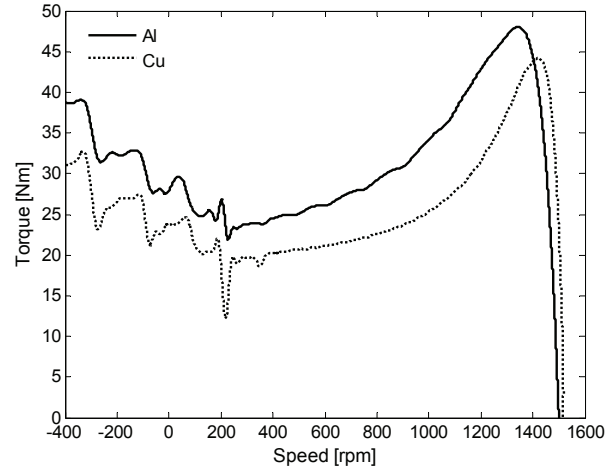


Fig. 7 Torque as a function of speed for the machine at 200 V.

The voltage is increased to 200 V, Fig. 7 shows the measured torque for the two rotors. The asynchronous torques of order 11 and 13 are now drastically increased in amplitude.

The harmonic torques counteracts the accelerating torque at higher speeds, resulting in a reduced pull out torque. The peak torque of the copper rotor relative to the aluminum rotor is now lower, indicating that the braking torque contribution from the harmonics are larger in the copper rotor.

Fig. 8 shows the obtained torque when starting at rated voltage. The machine is now saturated, which somewhat suppresses the characteristic forms of the asynchronous torques. Among the harmonic torques, order 11 seems to be the most dominating one, especially for the copper rotor. The 7th order may be larger but it is still difficult to observe due to the presence of the synchronous torque.

The pull-out torque of the copper rotor is 8 % less than the pull-out torque of the aluminium rotor. This implies that the inter-bar currents are causing even larger losses in the copper rotor than what the analytical model predicts.

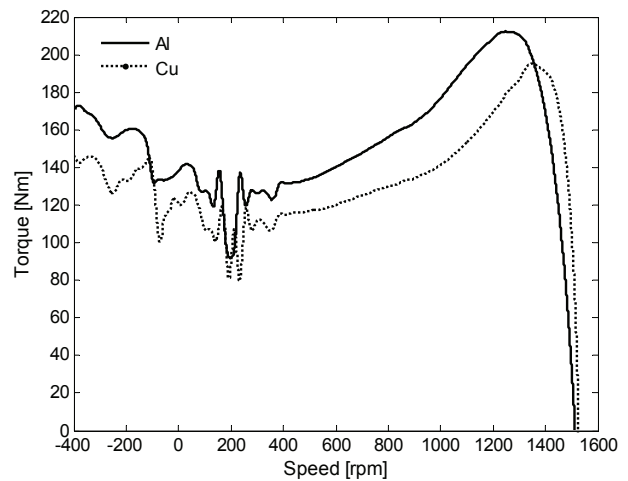


Fig. 8 Torque as a function of speed for the machine at 400 V.

V. CONCLUSIONS

Results from measurements have shown that the inter-bar resistivity is at least 10 times lower in cast copper rotors than in cast aluminium rotors. This has considerable influence on the amplitude of inter-bar currents. Simulations have shown that the magnitude of the braking torque from the harmonics is larger in the copper rotors than in the aluminium rotors. This is seen as reduced pull-out torque and increased stray-load losses in the machine.

Measurements have shown that the reduction of the pull-out torque is even larger than calculated from the model. The measured pull-out torque of the studied copper rotor was 8 % lower than for the equivalent aluminium rotor. Thereby, it can be concluded that the inter-bar currents have a considerable effect on motor performance, especially on machines with die cast copper rotors.

ACKNOWLEDGEMENT

This work has been carried out within the High Performance Electrical Machines and Drives program of the Center of Excellence in Electric Power Engineering at the Royal Institute of Technology in Stockholm.

REFERENCES

- [1] A. M. Odok, *Stray-load losses and stray torques in induction machines*, AIEE Trans. vol. 77, no. 4, page(s): 43-53, 1958.
- [2] K. Dabala, *A new experimental-computational method to determine rotor bar-iron resistance*, Proc. of ICEM, vol. II, page(s): 69-72, 1996.
- [3] K. Dabala, *Modified method to determine rotor bar-iron resistance in three-phase copper casted squirrel-cage induction motors*, Proc. of ICEM, page(s): 231-234, 2006.
- [4] A. Behdashti M. Poloujadoff, *A new method for the study of inter-bar currents in polyphase squirrel-cage induction motors*, IEEE Trans. vol. PAS-98, no. 3, page(s): 902-911, May/June 1979
- [5] C. Sadarangani, *Electrical machines – design and analysis of induction and permanent magnet motors*, ISBN 91-7170-627-5, KTH Högskolestryckeriet, Stockholm, 2000.
- [6] H.P. Nee, *On rotor slot design and harmonic phenomena of inverter-fed induction motors*, ISSN-1100-1631, KTH, TS- Tryck & Kopiering, Stockholm, 1996.